Talanta 88 (2012) 463–467

Contents lists available at SciVerse ScienceDirect

Talanta

journal homepage: www.elsevier.com/locate/talanta

A compact and highly sensitive light-emitting diode-induced fluorescence detector for capillary flow systems

Xuhui Geng[a,b], Dapeng Wu[a], Yafeng Guan[a,*]

[a] Department of Instrumentation & Analytical Chemistry, Key Lab of Separation Science for Analytical Chemistry of CAS, Dalian Institute of Chemical Physics, Chinese Academy of Sciences, 457 Zhongshan Road, Dalian 116023, China
[b] Graduate School of the Chinese Academy of Sciences, Beijing 100039, China

ARTICLE INFO

Article history:
Received 19 July 2011
Received in revised form 2 November 2011
Accepted 3 November 2011
Available online 9 November 2011

Keywords:
Light-emitting diode
Fluorescence detector
Compact

ABSTRACT

A compact and highly sensitive light-emitting diode-induced fluorescence detector (LED-FD) was constructed and evaluated. The LED excitation beam was restricted by a 200 μm diameter pinhole on a 55 μm thick lighttight film. The LED, excitation filter, pinhole, and capillary flow cell were placed tightly against each other without either optical lens or excitation fiber. The performance of the LED-FD was evaluated by flow injection analysis (FIA) of sodium fluorescein solution. The limit of detection (LOD) was determined as 0.75 nM (SNR = 3). Compared with our previous work, a 3.5-fold enhancement on the signal-to-noise ratio (SNR) was obtained. The system exhibited linear responses in the concentration range of 2–200 nM (R = 0.9993). The error of repeatability was within 2.0% R.S.D. on peak height in a ten-repeated injection of 5 nM solution. The reproducibility between devices was within 2.2% R.S.D. on peak height of 10 nM fluorescein solution. Finally, the LED-FD was compared with commercial fluorescence detector, and similar fluorescence signal intensity was obtained.

1. Introduction

Fluorescence detection has been one of the most sensitive and selective detection schemes available for capillary flow systems, such as flow injection analysis (FIA), capillary electrophoresis (CE), and microcolumn liquid chromatography (μ-LC) [1–3]. Light-emitting diode (LED) has many advantages including long lifetime, high stability, small in size, and low cost. Moreover, LED is commercially available at wavelengths ranging from deep-UV to near-IR regions. LED has been used as alternative light source in fluorescence detections [4–6]. Unfortunately, owing to its area source and incoherent characteristic, light emitted by an LED usually has a wide divergence angle. It is difficult to focus LED light beam to a small spot to match the inner diameter (i.d.) of a fused-silica capillary. So the excitation light intensity in a light-emitting diode-induced fluorescence detector (LED-FD) is usually under 0.1 $\mu W/\mu m^2$. It is at least ten times lower than that in a laser-induced fluorescence detector (L-FD) [7]. Generally, LEDs and lasers are different in nature. The common divergence angle is >20° for LEDs but ~0° for lasers. The Full Wave at Half Maximum (FWHM) at visible light is ~30 nm for LEDs, while for lasers it is ~0.1 nm. Therefore, the background noise in an LED-FD is generally several times higher than that in an L-FD [7]. All of these factors lead LED-FDs to a much poorer detection limit.

In order to achieve light focusing, optical lens were often preferred to be used in LED-FDs studies, e.g., lens group and objective [8–10]. It did bring some focusing effect, but increase optical path and reflectance, take a tedious calibration process, and show tight position tolerance. Further, it made the detection system complicated and bulky, which even offset the advantages of small size and low cost of LED itself. Compared with optical lens, excitation fiber was simple and flexible. It could restrict the spot size and divergence angle of LED beam strictly to its core diameter and aperture angle [11,12]. But only the LED beam within the aperture angle of the excitation fiber could be transmitted. The use of the excitation fiber also increased the length of optical path. Therefore, the light intensity at the detection cell was partly impaired. Recently, LED-FDs that were constructed by using optical lens system and excitation fiber together reached the sensitivity of 10^{-10} M [13,14].

In the present work, we intended to build a small and compact LED-FD of high sensitivity. Neither optical lens nor excitation fiber was used for LED coupling. Instead, all excitation components including LED, excitation filter, pinhole, and capillary were placed tightly against each other. This simple and compact configuration made the distance between LED source and detection cell as short as possible. Thus, the LED light could transfer to the detection cell to the upmost. The divergence angle of the LED and the diameter of

* Corresponding author.
E-mail addresses: guan_yafeng@yahoo.com.cn, kfguan@mail.dlptt.ln.cn (Y. Guan).

0039-9140/$ – see front matter © 2011 Elsevier B.V. All rights reserved.
doi:10.1016/j.talanta.2011.11.015

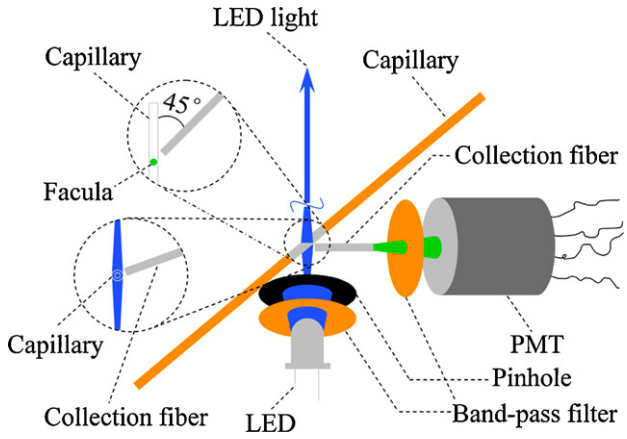

Fig. 1. Schematic diagram of the optical setup of the LED-FD system.

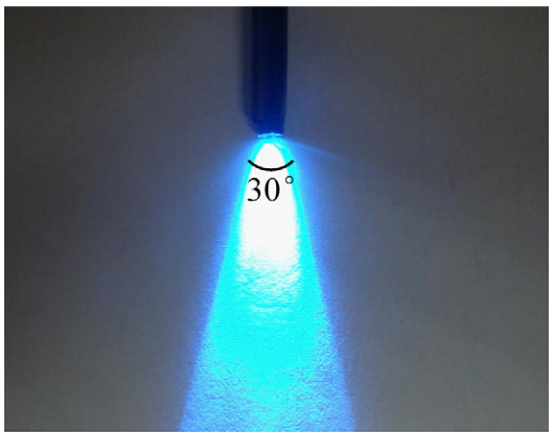

Fig. 2. Side view of the experimental LED beam.

the round pinhole were optimized carefully to achieve the highest SNR. The performance of the detector was evaluated by FIA method with sodium fluorescein solution.

2. Experimental

2.1. Chemicals and reagents

Sodium fluorescein was obtained from Sigma (USA), and was dissolved and diluted with deionized (DI) water to required concentrations. Bottles of sodium fluorescein stock solutions were wrapped carefully with black lighttight adhesive tape to prevent from photodegradation. Deionized water was used throughout experiments. Four kinds of amino acids, i.e., L-ornithine hydrochloride (L-orn), valine (Val), leucine (Leu), and phenylalanine (Phe) as well as FITC were purchased from Sigma.

2.2. Apparatus and equipments

A FIA system was constructed to evaluate the performance of the LED-FD. A fused silica capillary of 250 μm i.d., 365 μm o.d., with a 20 μm-polyimide coating (Xinnuo Optical Fiber Inc., Handan, China) was used, on which a 3 mm detection window was carefully burned and cleaned. A P230 HPLC pump (Elite Co. Ltd., Dalian, China) was used to pump the mobile phase. The mobile phase (deionized water) was treated with ultrasonic degassing before experiment. Injection was performed using a six-port injection valve (Valco Instruments, Houston, TX, USA) with a home-made 2 μL loop. Before the six-port injection valve, a commercial three-port manifold was used to finely adjust the flow rate to 10 μL/min.

2.3. Optical systems

The optical arrangement of the LED-FD is shown in Fig. 1. An ordinary LED (λ_{max}, 470 nm; diameter, 3 mm; divergence angle, 30°; power dissipation, 20 mA × 3.2 V; Shifeng Corp., China) was used as the excitation light source. The LED was aged for 150 h at 20 mA before use to eliminate the initial low frequency noise [15]. A 200 μm-diameter pinhole was punched on a 55 μm-thickness black lighttight adhesive tape (BTX-8923AD, Bitaixiang Electronic Corp. Ltd., China). This pinhole was used to define the size of the LED beam on capillary. An interference filter (BP 470 nm; FWHM 20 nm; Huibo Optical Corp. Ltd., China) was inserted between the LED and the pinhole to eliminate the interference of long-wavelength light from LED. An optical fiber (quartz core diameter, 300 μm; fluorine resin cladding, 15 μm; length, 45 mm; numerical aperture (NA), 0.37; Chunhui Inc., China) was used to collect fluorescence. The fluorescence passed through an interference filter (BP 530 nm; FWHM 30 nm; Huibo Optical Corp. Ltd., China), then was detected by a metal packaged mini PMT (H5784, Hamamatsu, Japan). The signal from the PMT was acquired by chromatographic workstation N2000 (Zhejiang University, China). The system was based on orthogonal optical arrangement. The excitation path is perpendicular to the plane of capillary and fluorescence collecting path. The angle between the capillary and the collection fiber was 45° which was demonstrated to be the optimum collection angle [15].

2.4. Derivatization and separation of amino acids

The four amino acids were labeled and separated. Each amino acid was prepared to 4 mM stock solution by DI water. A FITC solution of 4 mM in acetone (containing 1%, v/v pyridine) was used as labeling reagent. $Na_2B_4O_7$ solution of 10 mM (pH 9.0) was used as buffer. Every 1.2 mM amino acid labeling solution was prepared by mixing 60 μL stock solution of each amino acid with 60 μL labeling reagent and 80 μL borate buffer, and the resultant mixture was left in the dark overnight at room temperature. Then the four 1.2 mM FITC-labeled amino acid stock solutions were diluted to 1.2×10^{-5} M with borate buffer, and mixed by equal volume. Working solutions were prepared by diluting the mixed stock with borate buffer. Finally, the LED-FD was coupled with Agilent 1200 Series HPLC system. The separation was performed on CenturySIL C18 300A analytical column (150 mm × 4.6 mm × 5 μm, Johnsson Inc., Dalian, China) at room temperature. Isocratic elution was applied. The adopted chromatographic conditions were: mobile phase, 20 mM disodium (containing 5%, v/v methanol, pH 8.84): methanol = 72:28 (v/v); flow rate, 0.75 mL min^{-1}; injection volume, 20 μL.

3. Results and discussion

3.1. Selection of LED

An ordinary LED (20 mA) with a small divergence angle of 30° was chosen as the excitation light source. Its side view is shown in Fig. 2. It was operated at constant current mode. Its intensity fluctuation was 2×10^{-5}, and effective lifetime at constant driven current of 20 mA was 10^5 h. The maximum radiant power was 5 mW with the driven current of 20 mA at 25 °C. High-bright (HB) LEDs that have rated current as high as 700 mA are now available. But these HB LEDs need additional cooling modules to dispatch heat. They usually have a large emitting area as well as a highly divergence

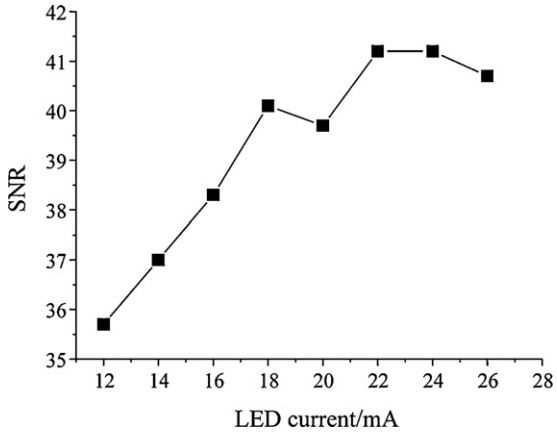

Fig. 3. Effect of LED driven current on SNR.

light beam. The light intensity per unit area of an HB LED is not higher than an ordinary Ø 3 mm LED. Because in this design, there was no optical lens or excitation fiber applied, the field angle of the light beam at the detection cell was just the divergence angle of the LED. In order to lower the background noise, the excitation light scattered to collection fiber should be as low as possible.

Depending on the modulating frequency, it was reported that the pulsed mode could enhance light intensity about 3 times higher. But this manner would accelerate LED aging and cause a poor reproducibility of experimental data. For long-term stability, constant current mode should be used. To ensure all the collected light was from the end face, the side face of the LED was wrapped carefully with black light-tight adhesive tape. In fact, all these measures applied on LED could lead to a similar effect as the focusing function of optical lens or fiber.

3.2. Effect of LED driven current

The effect of LED current on the performance of system was at driven current ranging from 12 mA to 26 mA, and the result is shown in Fig. 3. It revealed that the varying working current of LED had obvious impact on system performance. At first, the SNR increased with increase of driven current until 22 mA. After that, the SNR began to fall. It was possibly caused by over heating of LED's junction [6]. Considering the stability and lifetime of the LED, a long-term driven current of 20 mA (rating current) was applied.

The difference between junction temperature, ambient temperature and input thermal power can generate thermal stress which can impair the performance of LED [6]. The input power was 20 mA × 3.2 V, and the LED was operated at room temperature of 25 °C, the junction temperature was experimentally measured by a micro thermocouple. After the LED being illumined, its junction temperature increased gradually with time. After 5 min, it became stable at about 40 °C instead of over 125 °C of HB LED [12]. Therefore, the thermal stress here was not significant, although active cooling unit was not employed.

3.3. Selection of pinhole

The material used to make the pinhole should be able to block off most LED light out of pinhole area. In addition, the pinhole film should be as thin as possible, so LED could be as close as possible to the capillary detection area. As shown in Fig. 4, the black light-tight adhesive tape was chosen here as the substrate to make the pinhole. This tape was a 55 μm thick five-layer film, through which the transmission of LED light was less than 1×10^{-4}. This film was mainly made of polyethylene terephthalate (PET), which had very

Fig. 4. Configuration of the material used to make pinhole.

good long-term thermal and mechanical stability. The central black PET baseplate layer was fabricated by special printing techniques, and then processed by matte finish treatment. It had excellent light blocking characteristics. PET layers outside were affixed to the PET baseplate by the acrylic glue layer.

LED's divergent beam and polychromatic light often led to high background and noise. This was the dominant factor which affected the LOD of the detector [9]. In this design, the diameter of the round pinhole was a key factor to determine the overall performance of the detector. Small pinhole brought low background and noise but also low signal, while large was on the contrary. In order to reach the highest SNR, the pinhole diameter was optimized in the following.

Two optimizing principles were employed here. The first was that the optimum diameter of the pinhole should contribute the greatest transmission-to-reflection ratio on the outer wall of the detection window. The transmission excitation light produced fluorescence signal, while the reflection excitation light led to background noise. If the biggest incidence angle of excitation light beam on the detection window was 60°, the transmission-to-reflection ratio was nearly the greatest. This optimum angle of 60° could be deduced from the Fresnel's complete equation:

$$\rho(\lambda) = \frac{1}{2}\left[\frac{\sin^2(\theta_1 - \theta_2)}{\sin^2(\theta_1 + \theta_2)} + \frac{\tan^2(\theta_1 - \theta_2)}{\tan^2(\theta_1 + \theta_2)}\right], \quad (1)$$

where $\sin\theta_1/\sin\theta_2 = \eta_2/\eta_1$, θ_1 was the incidence angle, θ_2 was the refractive angle, η_1 was the refractive index of incidence media, and η_2 was the refractive index of refractive media. Fig. 5 illustrates how reflectance changed with the incidence angle for a monochromatic beam traveling through air–silica interface. It was obtained by numerical simulation of Fresnel's complete equation (1). When the incidence angle <60°, the reflectance was low and it changed slowly. When it was 60–90°, the reflectance increased rapidly till 100%. Thereby, the part of LED light with incidence angle smaller

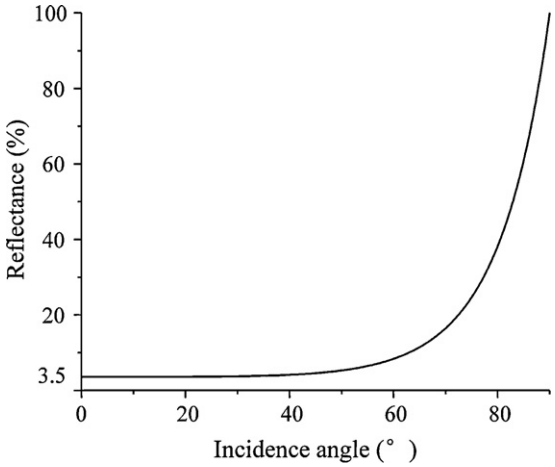

Fig. 5. Reflectance varies with incident angle for a monochromatic beam traveling through air (η = 1.000)–silica (η = 1.467) interface.

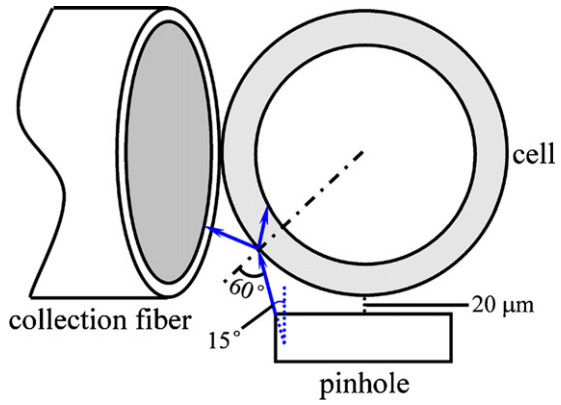

Fig. 6. Schematic diagram of the light path of the LED light through pinhole.

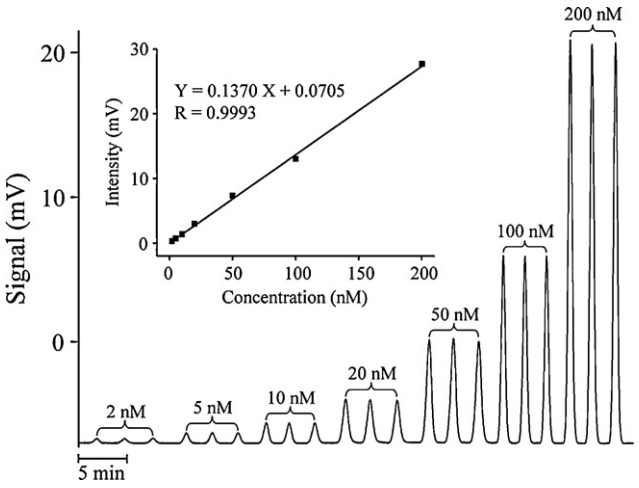

Fig. 7. Linear response of sodium fluorescein (2–200 nM) in flow injection mode. *Conditions*: flow rate, 10 μL/min; injection volume, 2 μL; PMT voltage, 600 V.

than 60° would contribute the greatest transmission-to-reflection ratio. The angle of 60° was chosen as approximate critical angle. Moreover, the secondary principle was that the pinhole should be shrunk till all the refractive light could irradiate the capillary inner volume (sample area). According to the two principles above, the optimum pinhole diameter was calculated to be 193.4 μm by ray tracing method, which is a basic method in optics domain to simulate optics process and calculate optics parameter. The schematic diagram of the light path is shown in Fig. 6. It simply based on Fresnel refraction and reflection law. In the experiment, the pinhole diameter of approximately 200 μm was fabricated by manually drilling on the black light-tight adhesive tape. Compared with other pinhole diameters, this value brought the highest SNR.

3.4. Effect of excitation filter

The excitation band pass filter was applied and about 3 times enhancement of SNR was achieved. The use of spectral filter in LED-FDs was investigated extensively by de Jong and Lucy [9]. The excitation filter can strongly eliminated the long wavelength light from LED. But it also brought two disadvantages: the reduced transmission of the LED light and the increased optical path. Our previous works had demonstrated that the attendance of excitation filter could improve the sensitivity of an LED-FD to about four times [12,16]. Thus, in this study, the excitation band pass filter was applied.

3.5. System characteristics

The performance of the LED-FD was evaluated in terms of the reproducibility of peak heights, response linearity, and the limit of detection (LOD) by FIA method. The sample was sodium fluorescein, which was a common fluorescence probe used to evaluate the capability of a fluorescence detector. The peak-to-peak noise level was about 47 μV under experimental conditions. The baseline drift was about 1 μV/min. The error of repeatability was within 2.0% R.S.D. on the peak height in a ten-repeated injection of 5 nM solution. The R.S.D. of reproducibility was 2.2%. The system exhibited a linear response in the concentration range of 2–200 nM (R = 0.9993) as shown in Fig. 7. Fig. 8 shows the image obtained with a 10 nM solution. From this figure, the LOD (SNR = 3) was estimated to be 0.75 nM, which was only 1/3.5 of our earlier report [11]. The size of the whole detector was only 9 cm × 9 cm × 4 cm ($W \times L \times H$), which was much less than the volume of conventional fluorometer or L-FD system.

We also tested a fused silica capillary of 100 μm i.d. on the system, yielding a LOD of 17 nM. Compared with the LOD of 0.75 nM on capillary of 250 μm i.d., it was 23 times higher. This phenomenon could be explained in two aspects. First, in theory, the sensitivity of this detector was in direct ratio to the detection volume. The optimum pinhole diameter varied with capillary i.d. in approximate ratio, which was mentioned above in the secondary principle for pinhole diameter selection. The excitation optical length was just the capillary i.d., and the detection volume was in approximate ratio to the cubic of capillary i.d. The detection volume ratio of the two capillaries was 2.5^3. Second, in practice, there was a discrimination effect in optical alignment to capillary i.d. The smaller the capillary i.d., the harder the alignment between pinhole and detection window, the worse the alignment result. For example, a little offset during the alignment might lead to a tiny change of SNR for bigger capillary i.d. as 250 μm. But the same offset would cause a great decrease of SNR for smaller capillary i.d. as 100 μm. Two reasons mentioned above worked together and resulted in sharp decrease of SNR from 250 μm to 100 μm capillary i.d.

A comparison of LOD of ten primary LED-FDs reported after 2005 is listed in Table 1. The literatures listed here were these aimed at the detector itself but not sample preconcentration or application. Because there had never been a standard evaluation conditions for LED-FD, the sensitivity was roughly estimated by us. For CE methods, because of the zone concentration effect, the SNR was generally enhanced by several times when the sample was prepared in a

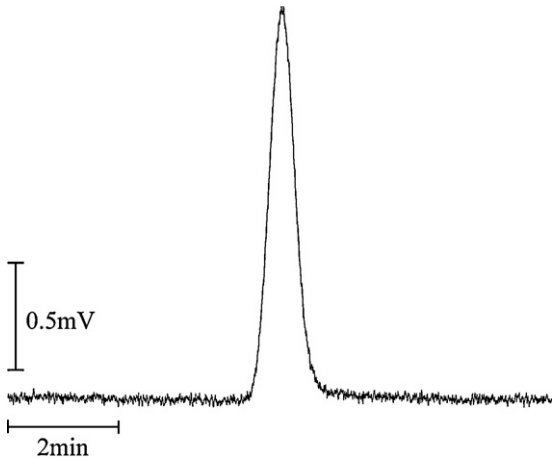

Fig. 8. Magnified peak profile of 10 nM sodium fluorescein solution. Conditions were the same as Fig. 7.

Table 1
Comparison of LOD of ten LED-FDs (sequence was roughly estimated by us).

LED	Focus	Collection	Evaluation	Sample	LOD (SNR = 3)	Literature
Ordinary, pulsed to 200 mA	Lens + gradient index lens + fiber	60× objective	CE	Fluorescein	0.29 nM	[14]
Ordinary, continuous	None	Fiber	FIA (no concentration)	Fluorescein	0.75 nM	Our work
Ordinary, continuous, increase luminance by 50%	Lens + gradient index lens + fiber	40× objective	CE	FITC-labeled L-asparagine	0.8 nM	[13]
High-bright, 150 mA, continuous	Fiber + RIMF	Fiber	CE	Fluorescein	1.5 nM	[12]
Ordinary, continuous, two LEDs	Fiber + windowless	Fiber	FIA (no concentration)	FITC	2.6 nM	[11]
Ordinary, continuous	Lenses + 20× objective	20× objective	CE	Fluorescein	3 nM	[9]
Ordinary, continuous, trunked	Fiber + RIMF	Fiber	CE	FITC	4 nM	[7]
Ordinary, continuous	Achromatic lenses	Fiber	CE	Fluorescein	5 nM	[16]
Ordinary, continuous	100× objective + fiber	100× objective	CE	FITC-labeled AAs	8 nM	[10]
Ordinary, continuous	Lens	25× ocular	CE (no concentration)	Fluorescein	0.92 μM	[15]

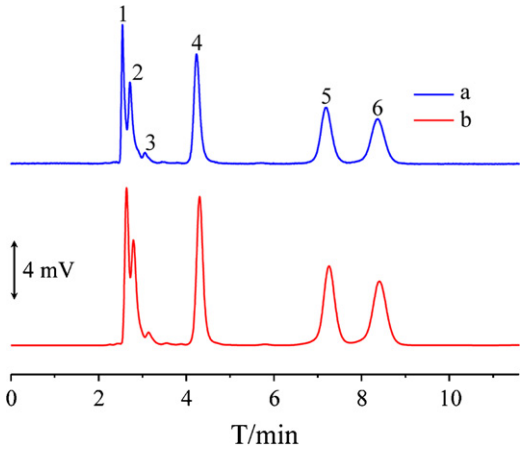

Fig. 9. HPLC chromatogram of FITC-labeled amino acids detected by our LED-FD (a) and Agilent G1321A FLD (b). Sample concentration: 0.1 μM; peak identification: 1–3, FITC-labeled L-ornithine hydrochloride; 4, FITC-labeled valine; 5, FITC-labeled leucine; and 6, FITC-labeled phenylalanine.

buffer much diluter than the running buffer [13,14]. For FIA methods, there is no such concentration effect, but there is a dilution effect instead [11]. Either the use of HB LEDs or pulse modulation mode driving to higher light intensity could enhance the SNR over several times [12,14]. And the use of refractive index matching fluid (RIMF) could increase the SNR over two times [7]. The data in Table 1 suggested that the LOD of our LED-FD could be further improved by applying brighter LED, pulse driving mode, and RIMF [12].

The system performance was compared directly with commercial Agilent G1321A FLD (fluorescence detector). Fig. 9 shows the chromatogram of four kinds of FITC labeled amino acids detected by the LED-FD and Agilent G1321A FLD. The migration times obtained by the two detectors were in good agreement. The LOD on our LED-FD was 1.7, 2.1, 4.1, and 5.1 nM for L-orn, Val, Leu and Phe, respectively, while on Agilent G1321A FLD was 7.4×10^{-11} M, 7.8×10^{-11} M, 1.4×10^{-10} M, and 1.8×10^{-10} M, separately. The peak heights on LED-FD were similar as those on Agilent G1321A FLD. But its noise was one order of magnitude higher than that of Agilent G1321A FLD. It was probably because the Agilent G1321A FLD employed pulse modulated technique (296 Hz), lock-in amplifier, low pass filter and reference system.

4. Conclusions

We have developed a compact and highly sensitive LED-FD for micro flow systems. The LED, excitation filter, pinhole, and capillary polyimide coating were placed side by side directly, and there were no optical lens or excitation fiber applied. In this method, LED of small divergence angle was chosen. The principle of optimization of the pinhole diameter was discussed. The LOD of 0.75 nM was among the lowest in the literatures. Although our LED-FD was not novel in its mechanism, under its very simple structure, its sensitivity surpasses most of other LED-FDs. It has the advantages of compact structure, no focusing adjustments, easy use and maintenance, and reasonable sensitivity, and low cost for application in micro flow systems, such as FIA, CE, and LC. We believe this study is of interest to currently working with LED-FD researchers.

Acknowledgements

This work was supported by the National Natural Science Foundation of China (Nos. 20635010, 21005080), Chinese Academy of Sciences (No. KZCX1-YW-14-3), and the Ministry of Science and Technology of China on High Tech Program (No. 2008AA09Z110).

References

[1] K. Tsunoda, T. Yagasaki, S. Aizawa, H. Akaiwa, K. Satake, Anal. Sci. 13 (1997) 757–764.
[2] S.L. Wang, X.J. Huang, Z.L. Fang, P.K. Dasgupta, Anal. Chem. 73 (2001) 4545–4549.
[3] X.W. Chen, J.H. Wang, Talanta 69 (2006) 681–685.
[4] A.E. Bruno, F. Maystre, B. Krattiger, P. Nussbaum, E. Gassmann, Trends Anal. Chem. 13 (1994) 190–198.
[5] S. Hillebrand, J.R. Schoffen, M. Mandaji, C. Termignoni, H.P.H. Grieneisen, T.B.L. Kist, Electrophoresis 23 (2002) 2445–2448.
[6] F. Yang, X.C. Li, W. Zhang, J.B. Pan, Z.G. Chen, Talanta 84 (2011) 1099–1106.
[7] J. Xu, S.H. Chen, Y. Xiong, B.C. Yang, Y.F. Guan, Talanta 75 (2008) 885–889.
[8] B.C. Yang, Y.F. Guan, Talanta 59 (2003) 509–514.
[9] E.P. de Jong, C.A. Lucy, Anal. Chim. Acta 546 (2005) 37–45.
[10] S.L. Zhao, H.Y. Yuan, D. Xiao, Electrophoresis 27 (2006) 461–467.
[11] J. Xu, B.C. Yang, H.Z. Tian, Y.F. Guan, Anal. Bioanal. Chem. 384 (2006) 1590–1593.
[12] J. Xu, Y. Xiong, S.H. Chen, Y.F. Guan, Talanta 76 (2008) 369–372.
[13] F. Huo, H.Y. Yuan, M.C. Breadmore, D. Xiao, Electrophoresis 31 (2010) 2589–2595.
[14] F. Huo, H.Y. Yuan, X.P. Yang, M.C. Breadmore, D. Xiao, Talanta 83 (2010) 521–526.
[15] F.B. Yang, J.Z. Pan, T. Zhang, Q. Fang, Talanta 78 (2009) 1155–1158.
[16] B.C. Yang, H.Z. Tian, J. Xu, Y.F. Guan, Talanta 69 (2006) 996–1000.